Least squares estimation of kinetic parameters in batch adsorption of phenol with confidence interval analysis

Yan Shao, Huiping Zhang, and Ying Yan[†]

School of Chemistry and Chemical Engineering, South China University of Technology, Guangzhou 510641, P. R. China

Abstract−Adsorption kinetics of phenol on granular coconut shell activated carbon and granular coal based activated carbon was investigated by the model of homogeneous surface diffusion plus external film mass transfer with the stirred batch adsorber. The model was solved numerically by finite element and the parameter estimation was performed with the nonlinear least squares method. Through the confidence interval analysis and evaluation of the error sum of squares, higher precision of the parameter estimates can be obtained by combining more decay curves; the decay curves with the different initial solution concentrations and adsorbent dosages can be well represented with identical film mass transfer coefficient and surface diffusivity, and the effect of surface adsorption coverage on the surface diffusivity is negligible in the adsorption systems. The values of the film mass transfer coefficient and surface diffusivity are in the order of magnitude 10^{-5} and 10^{-12}, respectively.

Key words: Batch Adsorption, Phenol, Confidence Interval, Surface Diffusion, Film Mass Transfer

INTRODUCTION

Adsorption on activated carbon is among the most widely used methods in the treatment of organic wastewaters [1,2]. Phenol and its derivatives are used in a number of applications, and as typical hazardous pollutants exist widely in those industrial effluents [3,4]. In the present study, phenol as a model adsorbate is used to reveal the problems in the adsorption kinetics. The kinetic parameters are very important in understanding the adsorption process mechanism and the design of adsorbers [5].

The batch adsorber method [6] is usually applied to measure adsorption equilibrium and kinetics. In the field of adsorption wastewater treatment, many publications involve the pseudo first/second-order rate model to fit the adsorption update curves [7-9]. The pseudo *p*th-order rate model may be expressed as

$$\frac{\partial \overline{q}}{\partial t} = k_{ps}(q_e - \overline{q})^p \tag{1}$$

The assumption of q_e being a constant allows Eq. (1) to be integrated directly and solved analytically. In fact, q_e is the adsorption amount equilibrated with the solution concentration during adsorption, and therefore it should be a function of time in a finite batch system. In that case solving Eq. (1) requires additional equations. The assumption of the pseudo model may cause the kinetic parameters k_{ps} and p to lose their physical significance, and it can be seen from the results [8,9] that the parameter k_{ps} fitted is dependent on the initial concentration of the solution and the adsorbent dosage.

The adsorption process includes the molecules diffusing into the adsorbent particles. The homogeneous surface diffusion model has been widely used to describe the process. Under the zero initial condition and the boundary condition of a step change of the solution

concentration surrounding the particles, the diffusion equation for the homogeneous particles can be solved analytically as follows [10]:

$$\frac{\overline{q}}{q_0} = 1 - \frac{6}{\pi^2}\sum_{k=1}^{\infty}\frac{1}{k^2}\exp\left(-\frac{k^2\pi^2 D_s t}{r_p^2}\right) \tag{2}$$

where q_0 is the adsorption amount equilibrated with the solution concentration of the step change. To regress the parameters linearly [7,8,11], Eq. (2) may be approximated by the linear relation of $\overline{q}/q_0$ vs $t^{1/2}$ or vs $\exp(-Bt)$, and it can be also seen from the results that the parameter*s* fitted are dependent on the initial concentration of the solution and the adsorbent dosage. However, in a batch adsorption experiment, it is required that the solution concentration changes with time during adsorption, for adsorption amount $\overline{q}$ is calculated by the change, and thus the step boundary condition cannot be satisfied. Moreover, the external film resistance should be considered in most experimental conditions. The resistance will induce a transient concentration around the particle surface. For a nonlinear batch system with transient solution concentration and the invasion of external film mass transfer, it is difficult to find an analytical solution of the system.

Yang et al. [12] briefly reviewed the models constructed by intra-particle diffusion plus external film mass transfer. The other consideration is whether the kinetic parameters are constant. Many researches have shown D_s is temperature-dependent and adsorbed phase concentration-dependent [13,14]. That will be dependent on the adsorption system.

The kinetic parameters in the batch adsorption should be independent of initial solution concentration and adsorbent dosage; otherwise when the equation is solved, the parameters should be considered as dependent variables which need extra correlations to represent these parameters. It is most crucial that the kinetic parameters related to initial solution concentration and adsorbent dosage may not be practically useful; for example, the kinetic parameters determined by batch adsorption experiments are used to simulate packed

[†]To whom correspondence should be addressed.
E-mail: yingyan@scut.edu.cn

beds.

Least squares estimation [15] is widely used to obtain the parameters in a nonlinear kinetic model, although other methods are found, such as diagrammatizing analytical technique [16]. The estimation, with the error sum of squares (ESS) as a criterion, searches the feasible parameters to minimize ESS. Obviously, more experimental data will yield larger ESS, yet the parameters estimated may be more credible, which seems conflicting. For one set of experimental data, more parameters in the model will decrease ESS, in which it should be asked if the parameters estimated are reliable. The confidence interval (CI) analysis will help to answer these questions, but publications about the kinetic parameter estimation rarely involve the analysis.

In the present article, we investigated adsorption of phenol on two kinds of activated carbons with batch adsorption experiments and the mathematical model of surface diffusion plus external film mass transfer. The concentration decay curves with different initial solution concentrations and adsorbent dosages were measured and used to estimate the kinetic parameters with the least squares method. CI analysis and ESS evaluation explain how the parameters estimated are affected by the different experimental conditions and the assumption of D_s changing with the surface coverage.

EXPERIMENTAL

1. Materials

The adsorbents used are granular coconut shell activated carbon (CSAC) and granular coal based activated carbon (CBAC) provided by Shanghai Xing Chang Activated Carbon Co., Ltd. (Shanghai, China). Prior to an experiment, the activated carbon was washed several times with distilled water to remove fines and leachable impurities, and dried at 110 °C for 24 h to constant weight.

Phenol used is of AR grade, supplied by Guangzhou Chemical Reagent Factory (Guangzhou, China).

The phenol concentration in aqueous solution was measured by UV spectrophotometry (VARIAN carry 50, U.S.) at wavelengths of 270 nm.

2. Adsorption Isotherms

Adsorption isotherms were determined with batch adsorption experiments. The batch adsorption was carried out in 250 mL conical flasks. 50 mL aqueous solution containing phenol from 200 mg/L to 2,500 mg/L, and the adsorbent (0.1 g) were added to the flasks. The flasks were sealed and placed in a thermostatic shaker to maintain temperature at 25.0 °C for 24 hours for reaching equilibrium. The initial and final concentrations of the phenol were measured to calculate the total amount adsorbed.

3. Adsorption Kinetics

The adsorption kinetic experiments were performed in a stirred batch adsorber. The adsorber is a 1 L round-bottomed glass vessel. The agitating impeller consisted of two flat blades of diameter 65 mm and height 10 mm, and located in the position of the blades at one-third of height from the vessel bottom. The impeller was driven by IKARW20 digital electric motor (Specimen Model Factory, Shanghai, China), and the agitation speed was controlled at 300 rpm. The adsorber was placed in a thermostat water batch to maintain the temperature of the system at 25.0 °C. 500 mL solution of desired concentration (500, 1,000, 1,500, 2,000 and 2,500 mg/L, respectively)

and a fixed amount of activated carbon particles (3.0, 6.0 and 9.0 g respectively) were used in the experiments. During adsorption, samples were withdrawn from the solution at certain time intervals and analyzed by the UV spectrophotometry.

THEORY

The mass transfer kinetics in the batch adsorption system is described by the homogeneous surface diffusion model, which is based on the following assumptions: (a) the particle of the adsorbent is supposed to be spherical and homogeneous, (b) intraparticle mass transfer is governed by surface diffusion, (c) external film mass transfer is expressed by linear driving force, (d) external mass transfer and intraparticle diffusion are continuous at the solid-liquid interface, (e) adsorption equilibrium with the adsorbate loaded on the surface occurs instantly, and (f) the temperature of the system remains constant during adsorption.

According to assumptions (a) and (b), the intraparticle diffusion equation may be represented by

$$\frac{\partial q}{\partial t} = \frac{1}{r^2}\frac{\partial}{\partial r}\left(r^2 D_s \frac{\partial q}{\partial r}\right) \tag{3}$$

According to (c) and (d), the mass transfer from the external film into the particle may be expressed as

$$\rho_s \frac{\partial \overline{q}}{\partial t} = k_f a_p (C_t - C_s) \tag{4}$$

According to the continuity of assumption (d), the boundary condition (B. C.) can be expressed as

$$D_s a_p \frac{\partial q}{\partial r}\bigg|_{r=r_p} = \frac{\partial \overline{q}}{\partial t} = \frac{k_f}{\rho_s} a_p (C_t - C_s) \tag{5}$$

and the symmetry yields

$$\frac{\partial q}{\partial r}\bigg|_{r=0} = 0 \tag{6}$$

For the fresh adsorbent the initial condition (I. C.) may be written as

$$q\big|_{t=0} = 0 \tag{7}$$

The solution concentration C_t can be obtained through the mass balance equation in solution

$$C_t = C_0 - \frac{\overline{q} \times W_s}{V_s} \tag{8}$$

The average adsorption amount $\overline{q}$ can be calculated by integration

$$\overline{q} = \frac{3}{r_p^3} \int_0^{r_p} q r^2 dr \tag{9}$$

C_s is the concentration on the surface of the adsorbent particles, which equilibrates with the adsorption amount $q(t, r_p)$ on the particle surface at t. C_s varies with t and can be calculated through the equilibrium equation. The equilibrium equation may be expressed with the Freundlich isotherm

$$q_e = K C_e^{1/n} \tag{10}$$

The following transformations are made to make the variables dimensionless:

$$R = \frac{r}{r_p}, \quad C_t^* = \frac{C_t}{C_0}, \quad C_s^* = \frac{C_s}{C_0}, \quad q^* = \frac{q}{q_0}, \quad \bar{q}^* = \frac{\bar{q}}{q_0}$$

where q_0 is equilibrium adsorption amount with C_0, calculated with Eq. (10). The kinetic parameters are transformed to

$$D_s^* = \frac{D_s}{r_p^2}, \quad k_f^* = \frac{k_f}{r_p}$$

Then the model can be written as

$$\frac{\partial q^*}{\partial t} = \frac{1}{R^2} \frac{\partial}{\partial R} \left(R^2 D_s^* \frac{\partial q^*}{\partial R} \right) \tag{11}$$

with I. C. and B. C.

$$q^* \big|_{t=0} = 0 \tag{12}$$

$$\frac{\partial q^*}{\partial R} \bigg|_{R=0} = 0 \tag{13}$$

$$\frac{q_0}{C_0} D_s^* \frac{\partial q^*}{\partial R} \bigg|_{R=1} = \frac{k_f^*}{\rho_s} (C_t^* - C_s^*) \tag{14}$$

The partial differential Eq. (11) is solved numerically by finite element scheme. The numerical solution yields the discrete data of the two dependent variables $C_t(t)$ and $q^*(t, R)$. By comparing with the experimental dimensionless concentration $C_{exp}^*(t_i)$, ESS may be calculated with

$$S = \sum_{i=1}^{m} (C_{exp}^*(t_i) - C_t^*(t_i))^2 \tag{15}$$

The parameters to be estimated, or decision variables, are denoted as

$$\mathbf{x} = (x_1, \ldots, x_j, \ldots, x_w) \tag{16}$$

where w is the number of the parameters. To estimate the parameters, an optimization algorithm is adopted to make ESS minimum

$$\min_{x} \{S\} \tag{17}$$

The simplex algorithm [15] is a direct search method which does not require derivatives $\partial S/\partial \mathbf{x}$. The trust-region algorithm and Levenberg-Marquardt algorithm [15] require numerical derivatives. These algorithms are used by turn to ensure the solution is optimal.

The above estimation, i.e., least squares estimation is a kind of point estimate, in which a single value is calculated as an estimate of the parameter. A confidence interval (CI) may be calculated along with the point estimate of the same parameter, to show the reliability of the estimate. To the parameter x_j (j=1, ..., w) and a given number α ($0 < \alpha < 1$), if statistics T_{1j} and T_{2j} are present and enable the probability

$$P(T_{1j} \leq x_j \leq T_{2j}) = 1 - \alpha \tag{18}$$

$[T_{1j}, T_{2j}]$ is CI of x_j at the confidence level $(1-\alpha)$, which means that, it is $(1-\alpha)100\%$ confident that the true value of the parameter x_j is in CI $[T_{1j}, T_{2j}]$. Larger CI indicates less precise estimate of the param-

eter. For a given significance level α, the CI may be evaluated by [15]

$$x_j \mp F^{-1}(P|v) \sqrt{c_{jj} S / v} \tag{19}$$

where $F^{-1}(P|v)$ is the inverse of Student's t cumulative distribution function at probability $P = 1 - \alpha/2$, and the degrees of freedom $v = m - w$. c_{jj} is the jth diagonal element of $(\mathbf{J}^T \mathbf{J})^{-1}$, where $\mathbf{J}$ is the Jacobian matrix of the fitted values with respect to the parameters, and its elements, i=1, ..., m, j=1, ..., w, are calculated by

$$j_{ij} = \frac{\partial C_t^*(t_i)}{\partial x_j} \tag{20}$$

In the present article, the solution of the model, the least squares estimation and CI calculation are programmed with the software package MATLAB.

RESULTS AND DISCUSSION

1. Physical Properties of GAC

The physical properties of CSAC and CBAC were determined with Micromeritics AutoPore IV 9500 (Micromeritics Instrument Corporation, U.S.) and ASAP 2010 (Micromeritics Instrument Corporation, U.S.), listed in Table 1. From the table, the Brunauer-Emmett-

Table 1. Physical properties of the activated carbons

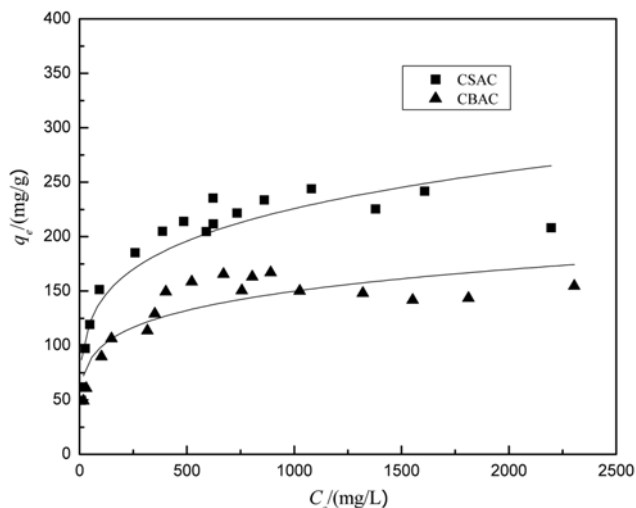| Property	CSAC	CBAC
Porosity	0.32	0.35
BET surface area (m^2/g)	906.3	562.0
Micropore volume (cm^3/g)	0.317	0.189
Mesopore volume (cm^3/g)	0.120	0.072
Pore diameter (nm)	1.9	1.8
Average particle diameter (mm)	1.5	2.4
Apparent particle density (kg/m^3)	718.6	852.4
Freundlich parameters K	54.96	42.96
n	4.890	5.530

Fig. 1. Equilibrium isotherms of phenol on CSAC and CSAC at 25.0 °C (Symbols: experimental; lines: Freundlich isotherms fitted).

Teller (BET) area of CSAC (906.3 m^2/g) is higher than that of CBAC (562.0 m^2/g). Also, the pore volume and the pore radius of CSAC are higher than that of CBAC.

The isotherms of phenol on CSAC and CBAC at 25.0 °C were measured and analyzed by Freundlich Eq. (10). The parameters were estimated by non-linear regression analysis using the least squares method. The fitted results are illustrated in Fig. 1 and listed in Table 1: the equilibrium adsorption amount of CSAC is greater than that of CBAC.

2. Kinetic Data Treatment

The adsorption kinetics of phenol on CSAC and CBAC at 25.0 °C were measured in a stirred batch adsorber with different adsorbent dosages and initial solution concentrations. For every adsorbent dosage and initial solution concentration, a concentration decay curve, i.e., a series of solution concentrations $C_{exp}(t)$ changing with time t, were measured. All the kinetic parameters can be estimated with the least squares method by only a single decay curve. However, to compare the estimating effect of experimental numbers on the estimation, more decay curves are put together in the estimation, in which it is supposed that the parameters are identical to all the curves. In such a way the parameters estimated are independent of the adsorbent dosage and initial solution concentration. To calculate CI, the confidence level $(1-\alpha)$ is set at 95% for all the cases.

3. Constant Surface Diffusivity

D_s is supposed as a constant in Eq. (11). Two parameters k_f^* and D_s^*, to be estimated, and Eq. (16) can be replaced by

$$\mathbf{x}=(k_f^*, D_s^*) \tag{21}$$

k_f and D_s on CSAC with five initial solution concentrations and three adsorbent dosages are estimated from one or more decay curves, listed in Table 2. In runs 1 to 7, a separate decay curve is used to estimate k_f and D_s, and different k_f and D_s are obtained for every experimental condition. Especially, the values of D_s are very discrete. In runs 8 and 9, three and five decay curves are used, respectively. CIs calculated from single decay curve are larger, and the more decay curves are involved, the smaller CI is obtained (an exception is the D_s CI of run 5 with the highest initial concentration), which means that more precise estimates of the parameters from more decay curves, although ESS is greater for more decay curves combined together. All experimental decay curves (seven in total) are put together to estimate the parameters, listed in Table 3. The smallest CI is obtained

Table 3. Estimated results of kinetic parameters on CSAC and CBAC for constant surface diffusivity from seven decay curves

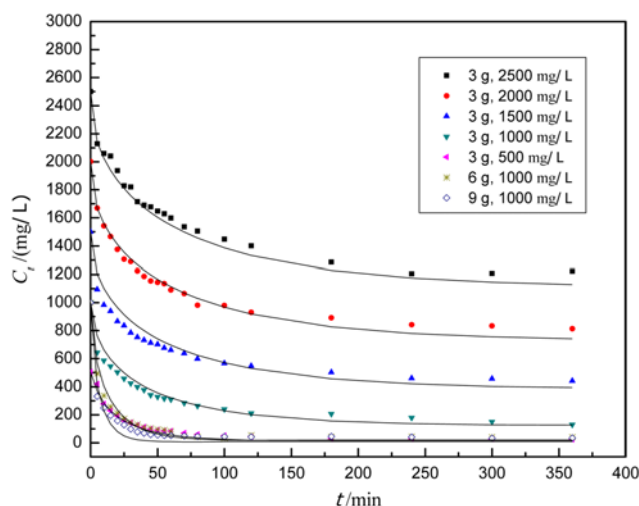| Kinetic parameter	CSAC	CBAC
$D_s\times10^{12}$ (m^2/s)	9.059	2.214
CI$\times10^{12}$ (m^2/s)	[8.879, 9.249]	[2.041, 2.386]
$k_f\times10^5$ (m/s)	3.129	1.310
CI$\times10^5$ (m/s)	[3.129, 3.135]	[1.310, 1.424]
ESS	0.2191	0.2547

Fig. 2. Effects of adsorbent dosage and initial solution concentration on the adsorption of phenol in CSAC (Symbols: experimental; lines: calculated with constant D_s).

in Table 3, indicating that the most precise kinetic parameters will be obtained with all seven decay curves together. Similar behavior on CBAC is obtained but is not listed in the present article for saving space.

The theoretical concentration decay curves for phenol on two kinds of carbon, calculated by the identical parameters for all curves, are compared with the experimental curves in Figs. 2 and 3. It is shown that the calculated decay curves agree well with the experimental curves. From results of Tables 2 and 3 and Figs. 2 and 3, k_f

Table 2. Estimated results of kinetic parameters on CSAC for constant surface diffusivity from single, three and five decay curves

Run no.	C_0 (mg/L)	W_s (g)	$D_s\times10^{12}$ (m^2/s)	CI$\times10^{12}$ (m^2/s)	$k_f\times10^5$ (m/s)	CI$\times10^5$ (m/s)	ESS
1	500	3	6.344	[5.307, 7.381]	3.132	[3.132, 3.133]	
2	1000	3	10.208	[8.916, 11.511]	3.762	[3.762, 3.763]	0.0227
3	1500	3	11.422	[9.847, 12.994]	3.100	[3.099, 3.100]	0.0230
4	2000	3	8.379	[8.517, 10.242]	3.109	[3.109, 3.110]	0.0079
5	2500	3	7.318	[6.794, 7.843]	3.929	[3.920, 3.940]	0.0031
6	1000	6	8.975	[7.198, 10.752]	3.184	[3.184, 3.185]	0.0255
7	1000	9	4.283	[3.252, 5.314]	3.190	[3.190, 3.191]	0.0288
8[a]			8.966	[7.985, 9.946]	3.119	[3.118, 3.119]	0.1018
9[b]			9.492	[8.733, 10.251]	3.119	[3.118, 3.119]	0.1634

[a]Decay curves of run no. 2, 5 and 7 are combined together to estimate

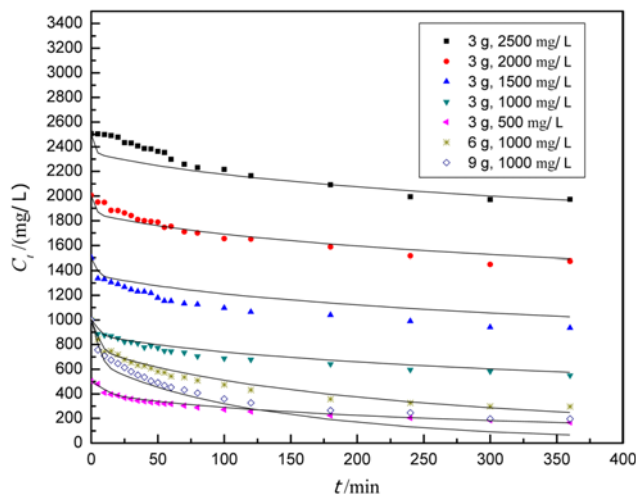[b]Decay curves of run no. 2, 3, 5, 6 and 7 are combined together to estimate

Fig. 3. Effects of adsorbent dosage and initial solution concentration on the adsorption of phenol in CBAC (Symbols: experimental; lines: calculated with constant D_s).

and D_s can be treated as independent of initial solution concentration and adsorbent dosage.

As seen in Table 3, the value of k_f on CSAC is greater than that on CBAC, which may be owing to smaller particle size of CSAC as shown in Table 1. Wakao and Funazkriz [17] and Hixson's empirical equation [18] show that k_f will increase with the decrease of particle size. The values of D_s in the order of magnitude 10^{-12} m²/s are consistent with the reported results [19,20]. Also, the value of D_s on CSAC is greater than that on CBAC. By comparing D_s and BET surface area for the activated carbons in Table 3 and 1, and from the literature [21,22], the adsorbent with the largest BET surface area has the greatest D_s. It may be because large BET surface area typically indicates more meso- or micropores in porous media, which generally represents larger effective diffusivity.

In the two processes of external film mass transfer and intraparticle surface diffusion, the parameter of the control process may be estimated with higher precision and thus with smaller CI. Therefore, by comparing CIs of k_f and D_s in Table 3, the contribution of the film mass transfer may be more significant than that of the surface diffusion, but the CI of D_s is not large enough to neglect the surface diffusion.

4. Variable Surface Diffusivity

The surface diffusivity may be dependent on the surface coverage when adsorption isotherm is nonlinear. Ash [23] compressed carbon powder into a tube and found that the surface diffusion increased rapidly as the monolayer coverage was approached. Yang [24] obtained the following equation for surface diffusivity, which allows for the second layer adsorption:

$$\frac{D_s}{D_s(0)} = \frac{1}{(1-\theta) + \theta\frac{\upsilon_1}{\upsilon_2}\exp[-(\Delta E_1 - \Delta E_2)/R_g T]} \quad (22)$$

$$\theta = \frac{\bar{q}}{q_{max}} \quad (23)$$

where q_{max} is the maximum adsorption amount, which can be regarded as q_m obtained from Langmuir isotherm equation:

$$q_e = \frac{q_m b C_e}{1 + b C_e} \quad (24)$$

q_{max} of CSAC and CBAC are 233.23 mg/g and 160.86 mg/g, respectively.

Since the experimental temperature is fixed, Eq. (22) can be simplified as

$$D_s = \frac{k_1}{1 - k_2\theta} \quad (25)$$

Another expression for correlating D_s and θ, as proposed in [14], is in the form of a power function,

$$D_s = a_1 \theta^{a_2} \quad (26)$$

In both cases, three parameters to be estimated, and Eq. (16) can be replaced by, respectively,

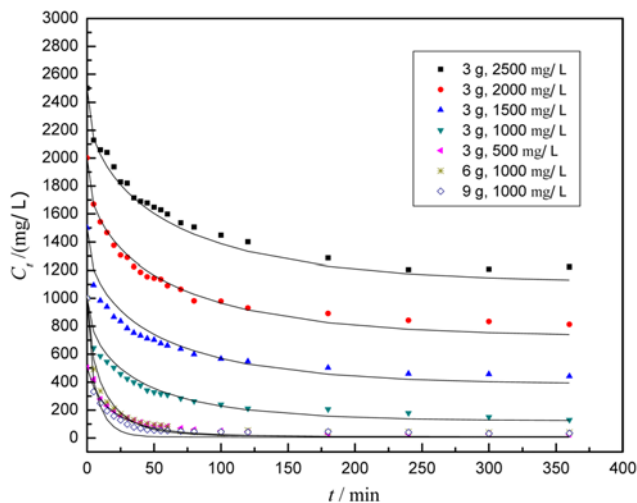$$\mathbf{x} = (k_f^*, k_1, k_2) \quad (27)$$

Fig. 4. Effects of adsorbent dosage and initial solution concentration on the adsorption of phenol in CSAC (Symbols: experimental; lines: calculated with variable D_s by Eq. (25)).
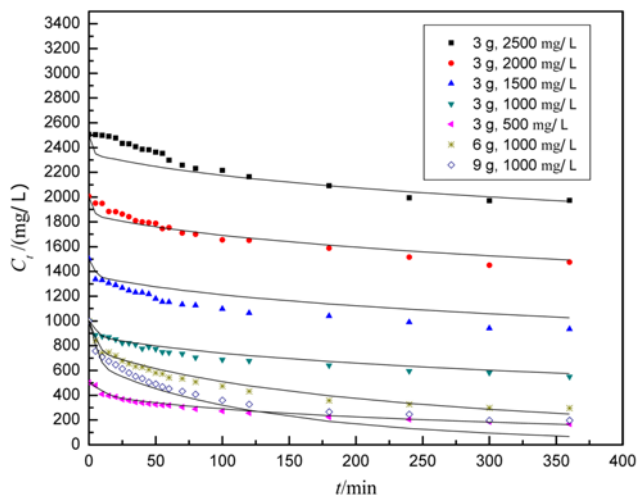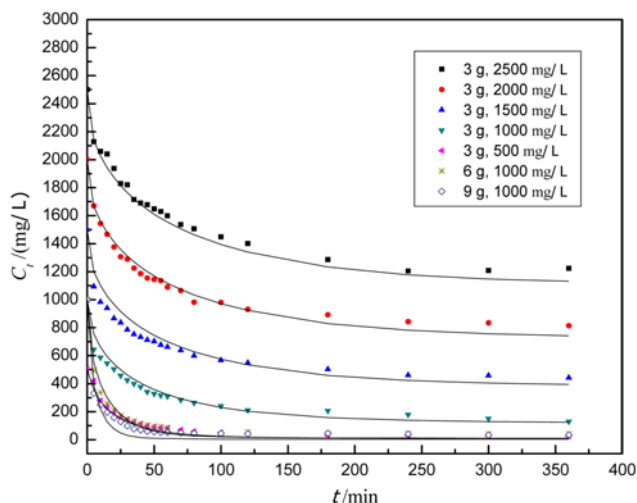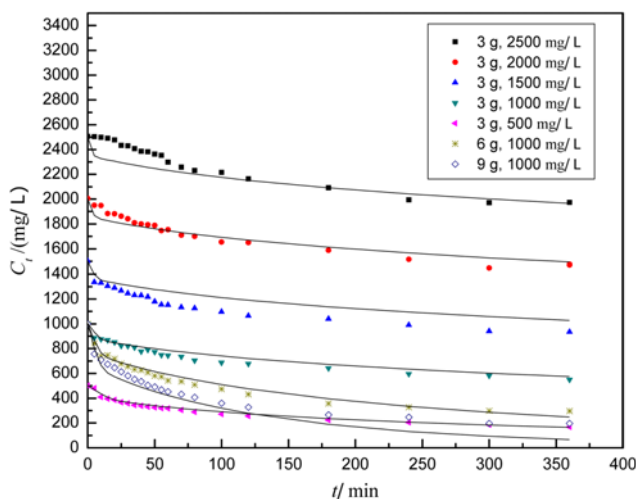

Fig. 5. Effects of adsorbent dosage and initial solution concentration on the adsorption of phenol in CBAC (Symbols: experimental; lines: calculated with variable D_s by Eq. (25)).

Fig. 6. Effects of adsorbent dosage and initial solution concentration on the adsorption of phenol in CSAC (Symbols: experimental; lines: calculated with variable D_s by Eq. (26)).

Fig. 7. Effects of adsorbent dosage and initial solution concentration on the adsorption of phenol in CBAC (Symbols: experimental; lines: calculated with variable D_s by Eq. (26)).

$$\mathbf{x}=(k_f^*, a_1, a_2) \qquad (28)$$

In the estimation, D_s in Eq. (11) is changed with t and R, represented by Eq. (25) or (26). The results are listed in Tables 4 and 5. The comparison of the calculated decay curves with the experimental decay curves is illustrated in Figs. 4 to 7, which shows good agreement between the calculated and experimental curves.

The changing trends of D_s with the changes of θ in two kinds of carbons are shown in Figs. 8 and 9. D_s slightly increases with the increase of θ. During the process of adsorption, the adsorbed molecules first occupy high-energy sites and then low-energy sites. The diffusion rate of the molecules will be faster in low-energy sites than in high-energy sites since the binding force is lower [25]. The surface diffusion is attributed to loosely bounded molecules. That is the reason why D_s increases with surface loading.

However, CIs of k_2 in Table 4 and a_2 in Table 5 are almost symmetric about zero, which indicates that k_2 and a_2 may approach zero
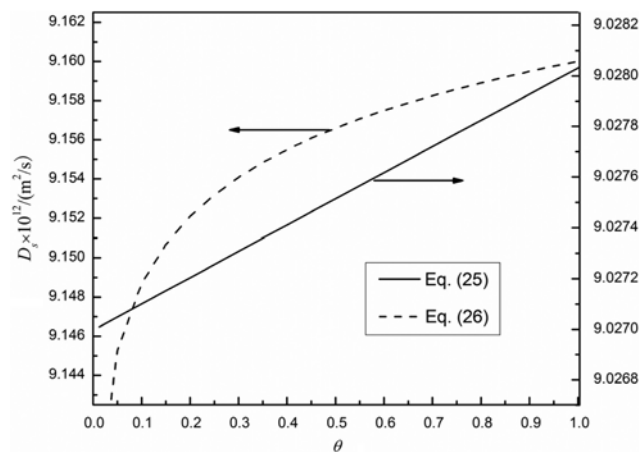

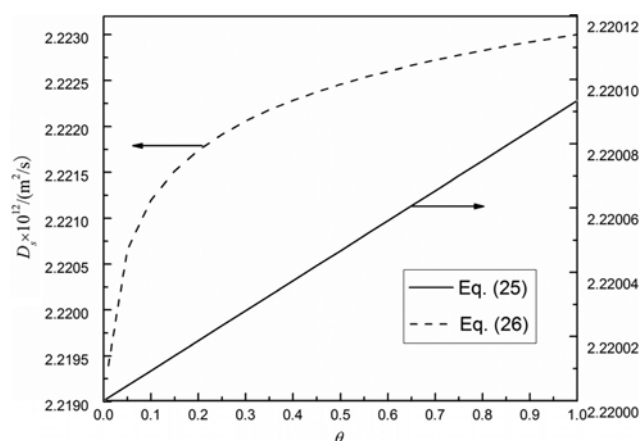
Fig. 8. D_s changes with θ on CSAC.

Fig. 9. D_s changes with θ on CBAC.

Table 4. Estimated results of kinetic parameters for varied surface diffusivity by Eq. (25) from seven decay curves

Kinetic parameter	CSAC	CBAC
$k_1 \times 10^{12}$ (m²/s)	9.027	2.220
$CI \times 10^{12}$ (m²/s)	[8.376, 9.678]	[2.045, 2.395]
$k_2 \times 10^4$	1.146	0.4208
$CI \times 10^2$	[−0.399, 0.422]	[−4.690, 4.698]
$k_f \times 10^5$ (m/s)	3.136	1.359
$CI \times 10^5$ (m/s)	[3.176, 3.176]	[1.357, 1.359]
ESS	0.2188	0.2547

Table 5. Estimated results of kinetic parameters for varied surface diffusivity by Eq. (26) from seven decay curves

Kinetic parameter	CSAC	CBAC
$a_1 \times 10^{12}$ (m²/s)	9.160	2.223
$CI \times 10^{12}$ (m²/s)	[7.171, 11.115]	[1.236, 3.250]
$a_2 \times 10^4$	5.367	3.525
CI	[−0.174, 0.194]	[−0.291, 0.292]
$k_f \times 10^5$ (m/s)	3.099	1.313
$CI \times 10^5$ (m/s)	[3.099, 3.100]	[1.308, 1.318]
ESS	0.2189	0.2539

at the given confidence level. If k_2 and a_2 approach zero, from Eqs. (25) and (26), the model of variable surface diffusivity will degenerate into that of constant surface diffusivity. Comparing the results in Table 3 with Tables 4 and 5, ESS cannot be decreased significantly by introducing variable surface diffusivity. Therefore it is reasonable to regard D_s as a constant.

Comparing the results in Tables 3-5, the values of k_f on the same kind of carbon are very close regardless of whether the surface diffusivity is variable or not.

CONCLUSION

The adsorption isotherms of phenol in aqueous solution on CSAC and CBAC can be fitted by the Freundlich equation. The homogeneous surface diffusion model based on external mass transfer and surface diffusion can well predict the concentration decay curves with different initial concentrations and adsorbent dosages. CI analysis and ESS evaluation indicate that higher precision of the parameter estimates can be obtained by combining more decay curves, the decay curves with the different experimental conditions can be well represented with identical film mass transfer coefficient and surface diffusivity, and the effect of surface adsorption coverage on the surface diffusivity is negligible in the present studied system.

ACKNOWLEDGEMENT

NOMENCLATURE

a_1, a_2 : constant in Eq. (26)
a_p　　: external surface area per unit particle volume [m^2/m^3]
b　　: constant in Langmuir isotherm [L/mg]
B　　: constant
c_{jj}　　: jth diagonal element
C_0　　: initial phenol concentration [mg/L]
C_e　　: liquid-phase phenol concentration at equilibrium [mg/L]
C_s　　: liquid-phase phenol concentration at particle surface [mg/L]
C_t　　: liquid-phase phenol concentration at t [mg/L]
D_s　　: surface diffusivity [m^2/s]
F　　: Student's t cumulative distribution function
J　　: Jacobian matrix
k_1, k_2 : constant in Eq. (25)
k_f　　: film mass transfer coefficient [m/s]
k_{ps}　　: constant of pseudo pth-order rate model [s^{-1}]
K　　: constant in Freundlich isotherm
m　　: the number of experimental data
n　　: constant in Freundlich isotherm
p　　: order of pseudo pth-order rate model
P　　: probability
q　　: adsorption amount [mg/g]
q_0　　: equilibrium adsorption amount with C_0 [mg/g]
q_e　　: equilibrium adsorption amount [mg/g]

q_m　　: constant in Langmuir isotherm [mg/g]
q_{max}　: maximum adsorption amount [mg/g]
$\overline{q}$　　: average adsorption amount [mg/g]
r　　: radial coordinate for particle [m]
r_p　　: particle radius [m]
R_g　　: gas constant [=8.314 J/mol/K]
S　　: error sum of squares, dimensionless
t　　: time [s]
T_{1j}, T_{2j} : confidence interval of parameter j
υ_1, υ_2 : vibration frequencies of the first and second layers
v　　: degrees of freedom
V_s　　: volume of solution [L]
w　　: the number of parameters
W_s　　: mass of adsorbent [g]
x　　: parameters (to be) estimated
$\Delta E_1, \Delta E_2$: heats of adsorption for the first and second layers [kJ/mol]

Greek Symbols
α　　: significance level, dimensionless
θ　　: surface adsorption coverage, dimensionless
ρ_s　　: apparent density of adsorbent [kg/m^3]

REFERENCES

1. Y. T. Hung, H. H. Lo, L. K. Wang, J. R. Taricska, K. H. Li, *Granular Activated Carbon Adsorption*, in: L. K. Wang, Y. T. Hung, N. K. Shammas (Eds.), *Physiochemical treatment processes*, Vol. 3, Handbook of Environmental Engineering, Humana Press Inc., Totowa, NJ (2005).
2. Y. T. Hung, H. H. Lo, L. K. Wang, J. R. Taricska, K. H. Li, *Powdered Activated Carbon Adsorption*, in: L. K. Wang, Y. T. Hung, N. K. Shammas (Eds.), *Advanced physicochemical treatment processes*, Vol. 4, Handbook of Environmental Engineering, Humana Press Inc, Totowa, NJ (2005).
3. S. H. Lin and R. S. Juang, *J. Environ. Manage.*, **90**, 1336 (2009).
4. A. Dabrowski, P. Podkoscielny, Z. Hubicki and M. Barczak, *Chemosphere*, **58**, 1049 (2005).
5. D. O. Cooney, *Adsorption design for wastewater treatment*, 5th Ed., CRC Press LLC, New York (1999).
6. D. D. Do, *Adsorption analysis: Equilibria and kinetics*, 9th Ed., Imperial College Press, London (1998).
7. G. Crini and P. M. Badot, *Prog. Polym. Sci.*, **33**, 399 (2008).
8. B. A. Fil, R. Boncukcuolu, A. E. Yilmaz and S. Bayar, *Korean J. Chem. Eng.*, **29**, 1232 (2012).
9. R. O. Perez, R. L. Ramos, J. M. Barron and R. M. G. Coronado, *J. Colloid Interface Sci.*, **364**, 195 (2011).
10. D. M. Ruthven, *Principles of adsorption and adsorption processes*, Wiley, New York (1984).
11. L. M. Cotoruelo, M. D. Marques, J. Rodrýguez-Mirasol, T. Cordero and J. J. Rodrýguez, *Ind. Eng. Chem. Res.*, **46**, 2853 (2007).
12. X. Y. Yang, S. R. Otto and B. A. Duri, *Chem. Eng. J.*, **94**, 199 (2003).
13. I. Neretniekst, *Chem. Eng. Sci.*, **31**, 465 (1976).
14. M. Suzuki and T. Fujii, *AIChE J.*, **28**, 380 (1982).
15. G. A. F. Seber and C. J. Wild, *Nonlinear regression*, Wiley, Hoboken, NJ (2003).
16. J. Fujiki, N. Sonetaka, K.-P. Ko and E. Furuya, *Chem. Eng. J.*, **160**,

683 (2010).

17. N. Wakao and T. Funazkri, *Chem. Eng. Sci.*, **33**, 1375 (1978).

18. W. Hixson and S. J. Baum, *Ind. Eng. Chem.*, **33**, 478 (1941).

19. G. McKay, *Chem. Eng. J.*, **81**, 231 (2001).

20. K. Satoh, H. J. Fan, H. Hattori, K. Tajima and E. Furuya, *J. Hazard. Mater.*, **155**, 397 (2008).

21. M. Streat, J. W. Patrick and M. J. Camporro Perez, *Water Res.*, **29**, 467 (1995).

22. V. C. Srivastava, M. M. Swamy, I. D. Mall, B. Prasad and I. M. Mishra, *Colloids Surf.*, **A 272**, 89 (2006).

23. R. Ash, R. M. Barrer and C. G. Pope, *Proc. Roy. Soc.*, **271**, 1 (1963).

24. R. T. Yang, J. B. Fenn and G. L. Haller, *AIChE J.*, **19**, 1052 (1973).

25. D. C. K. Ko, J. F. Porter and G. McKay, *Chem. Eng. Sci.*, **60**, 5472 (2005).